

## Evolution of Metals and Stars in Damped Lyman-Alpha Galaxies

Varsha P. Kulkarni

*University of South Carolina, Dept. of Physics and Astronomy,  
Columbia, SC 29208, U.S.A.*

**Abstract.** Damped Lyman-alpha absorbers in quasar spectra provide a unique tool to directly measure the abundances of elements in galaxies at redshifts  $0 < z < 5$ , and hence probe the chemical evolution of galaxies over  $> 90\%$  of the age of the Universe. Since cosmic chemical evolution models predict the global metallicity of galaxies to increase with time, it is of great interest to determine whether DLAs actually show such a trend. We discuss statistical analysis of existing DLA Zn data to examine the metallicity-redshift relation, and a comparison of the observed data with models of cosmic chemical evolution. We also describe efforts to expand the DLA abundance sample at  $z < 1.5$ , where the current data are particularly sparse. Finally, we discuss emission-line imaging studies of the absorber galaxies and compare constraints on their star formation rates with models based on the global star formation history.

### 1. Introduction

The damped Lyman-alpha (DLA) absorption systems in quasar spectra have high H I column densities  $N_{\text{HI}} \geq 2 \times 10^{20} \text{ cm}^{-2}$ , and contain most of the neutral gas in galaxies, nearly enough to form all of the stars visible today (Wolfe et al. 1995). DLAs are therefore expected to shed light on the history of star formation and heavy element production in galaxies. Furthermore, DLAs are selected only by the presence of high H I column density, regardless of the apparent brightness of the underlying galaxy. Therefore they are expected to offer a relatively unbiased representation of normal galaxies.

The exact nature of DLAs and their relation to present-day galaxies is not quite clear. But DLAs are presently our principal source of information about the chemical content of normal high- $z$  galaxies, since spectroscopic studies have yielded abundances for a large range of elements in a substantial number of DLAs. Several emission-line imaging searches for DLAs have also tried to constrain the star formation rates in these objects. The combination of spectroscopic and imaging information can make DLA observations a powerful tool for understanding the history of element production and star formation in galaxies.

### 2. Evolution of Metallicity

#### 2.1. Constraints from the Existing Data

Several studies of element abundances in DLAs have been carried out using data from 4-m and 8-m class optical telescopes (e.g., Meyer, Welty, & York 1989; Lu

et al. 1996; Kulkarni et al. 1996; Kulkarni, Fall, & Truran 1997; Pettini et al. 1994, 1997; Prochaska & Wolfe 1999, 2000; Prochaska et al. 2001, 2003; and references therein). Zn is considered a good probe of the total (gas + solid phase) metallicity in DLAs because Zn tracks Fe in most Galactic stars, it is undepleted on interstellar dust grains, and the lines of the dominant ionization species Zn II are often unsaturated. The  $N_{\text{HI}}$ -weighted mean metallicity,

$$\bar{Z} = \frac{\sum N(\text{Zn II})_i / \sum N(\text{HI})_i}{(\text{Zn/H})_{\odot}} Z_{\odot}, \quad (1)$$

is a good measure of the global mean metallicity (Kulkarni & Fall 2002).

Most cosmic chemical evolution models ranging from analytical studies to hydrodynamical simulations predict the global metallicity to rise from nearly zero at high  $z$  to nearly solar at  $z = 0$  (e.g., Malaney & Chaboyer 1996; Pei & Fall 1995; Pei, Fall, & Hauser 1999; Somerville et al. 2001; Tissera et al. 2001). The present-day mass-weighted mean metallicity of local galaxies is indeed nearly solar (e.g., Kulkarni & Fall 2002). If DLAs trace an unbiased sample of normal galaxies, their interstellar mean metallicity may also be expected to rise with time. It is therefore of great interest to ask whether or not DLAs actually show this trend. Surprisingly, there has been great debate about this issue, with most studies advocating no evolution in the global mean metallicity (Pettini et al. 1997, 1999; Prochaska & Wolfe 1999; Vladilo et al. 2000; Prochaska & Wolfe 2000; Savaglio 2000; Prochaska et al. 2001; Prochaska & Wolfe 2002).

We have examined this question by compiling 57 DLA Zn measurements for  $0.4 < z < 3.4$  from the literature (36 detections and 21 limits; Kulkarni & Fall 2002). We applied a variety of statistical techniques, including a binned linear  $\chi^2$  fit to  $\bar{Z}$  vs.  $z$ , an unbinned  $N(\text{HI})$ -weighted nonlinear  $\chi^2$  fit to an exponential relation, survival analysis to treat limits on Zn, and a comparison of data with chemical evolution models. Fig. 1 shows the  $N(\text{HI})$ -weighted mean metallicity  $\bar{Z}$  vs. redshift relation. Treating limits with survival analysis, the slope of the metallicity-redshift relation is  $-0.26 \pm 0.10$ , consistent at the  $\approx 2 - 3\sigma$  level both with model predictions ( $-0.25$  to  $-0.61$ ) and with no evolution. Recently, Prochaska et al. (2003) have reported a similar value for this slope ( $-0.26 \pm 0.07$ ) using Zn data in 11 DLAs together with Fe, Si, S, or O data for 114 other DLAs. These studies suggest that there may be some metallicity evolution in DLAs.

## 2.2. Improving the Statistics at $z < 1.5$

The main reason for the large uncertainty in the slope of the metallicity-redshift relation is the small number of measurements, especially at  $z < 1.5$ . Most previous DLA Zn studies have focused on  $z > 1.5$  because the Zn II  $\lambda\lambda$  2026, 2062 lines lie in the ultraviolet (UV) for  $z < 0.6$ , and the Lyman- $\alpha$  line lies in the UV for  $z < 1.6$ . For  $0.6 < z < 1.3$ , the Zn II lines can be accessed with ground-based telescopes, but lie at blue wavelengths where most spectrographs have lower sensitivity. It is very important to obtain more data at  $z < 1.5$ , because this regime spans  $\sim 70\%$  of the age of the Universe (for  $\Omega_m = 0.3$ ,  $\Omega_{\Lambda} = 0.7$ ). The low- $z$  data have great leverage on the slope of the metallicity-redshift relation, and can clarify the relation of DLAs to present-day galaxies.

To improve the statistics of the metallicity-redshift relation at intermediate redshifts, we have recently started a survey of element abundances for DLAs

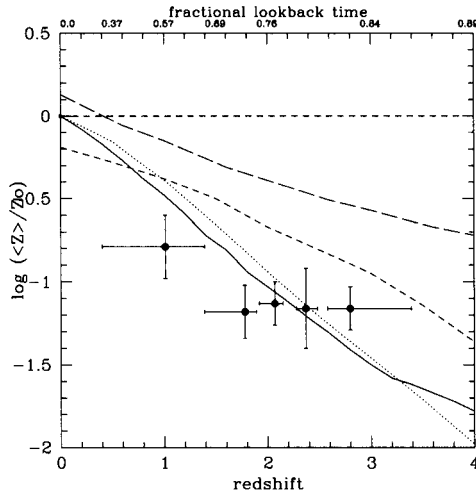


Figure 1.  $N(\text{HI})$ -weighted mean Zn metallicity vs. redshift for DLAs (Kulkarni & Fall 2002). Vertical error bars denote  $1\sigma$  uncertainties. Horizontal bars denote redshift spreads in each bin. Short-dashed, dotted, solid, and long-dashed curves show, respectively, the mean metallicity in models of Malaney & Chaboyer (1996), Pei & Fall (1995), Pei et al. (1999), and Somerville et al. (2001). The nonlinear scale on the top  $x$ -axis denotes fractional look-back time for  $\Omega_m = 0.3$  and  $\Omega_\Lambda = 0.7$ .

at  $0.6 < z < 1.5$  using the blue channel spectrograph on the Multiple Mirror Telescope (MMT). These spectra have resolution of  $\approx 75 \text{ km s}^{-1}$ , while the S/N near the Zn II  $\lambda 2026$  line is 25–130 for most objects. A wide range of Zn II line strengths is seen among the DLAs in our sample (Khare et al. 2004).

We are also carrying out a study of element abundances in DLAs at  $0.1 < z < 0.5$  with the Hubble Space Telescope. Most of these have  $\log N_{\text{HI}} > 20.9$  and are relatively important in determining the  $N_{\text{HI}}$ -weighted mean metallicity at low redshifts. The observations are being obtained with the Space Telescope Imaging Spectrograph (STIS) CCD and near-UV Multi-Anode Micro-channel Array (MAMA), at dispersions of 0.09 or 0.15  $\text{\AA}$ , and are being analyzed with IRAF/STSDAS. Together, our MMT and HST data have so far doubled the  $z < 1.5$  DLA Zn sample. These and future data at  $z < 1.5$  will help to clarify whether or not the global mean metallicity in DLAs shows evolution.

### 3. Star Formation History

Closely related to the history of metal production is the history of star formation. The cosmic star formation history has been estimated on the basis of deep galaxy imaging surveys such as the Canada-France Redshift Survey (Lilly et al. 1996) and the Hubble Deep Field (HDF; Madau et al. 1996, 1998). It is interesting to compare the star formation history of DLAs to the global star formation history.

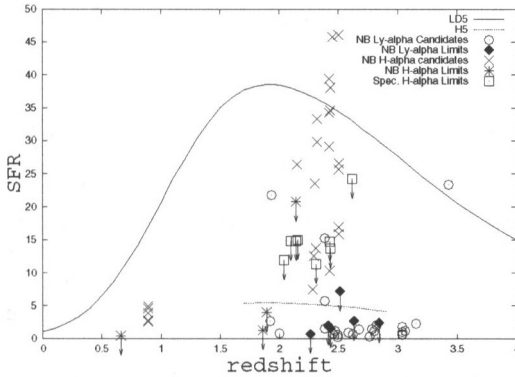


Figure 2. Measurements of SFRs (in  $M_{\odot} \text{ yr}^{-1}$ ) for quasar absorption selected objects, based on narrow-band imaging and spectroscopic searches for Ly- $\alpha$  and H- $\alpha$  emission lines. See text for further details.

### 3.1. Emission-line Imaging Studies of DLAs

One way to estimate the star formation rates (SFRs) in DLAs is by direct imaging in emission lines such as Ly- $\alpha$  or H- $\alpha$  commonly found in star-forming regions. The H- $\alpha$  line, although intrinsically weaker than Ly- $\alpha$ , is less susceptible to effects of dust attenuation. However, the imaging of DLAs is in general difficult because of the possibility of a small angular separation between the quasar and the foreground absorbing galaxy. High-resolution studies with the Hubble Space Telescope have been carried out for some DLAs. For the low- $z$  DLAs, a variety of morphologies has been observed. For high- $z$  DLAs ( $z \geq 1.5$ ), the situation remains unclear. Most attempts to detect and spectroscopically confirm high- $z$  DLA galaxies with  $z_{\text{abs}} < z_{\text{em}}$  have been unsuccessful.

To detect the underlying galaxies and measure their SFRs, we are carrying out deep imaging studies of high-redshift absorbers using HST and ground-based facilities. With the Near Infrared Camera and Multi-Object Spectrograph (NICMOS) on the HST, we have obtained diffraction-limited continuum and H- $\alpha$  images of DLAs with  $z \approx 1.9$ , at a FWHM of 0.15-0.17'' (Kulkarni et al. 2000, 2001). The highly stable and reproducible point spread function (PSF) of the HST NICMOS enabled us to search for absorbing galaxies as close as  $\sim 0.2''$  from the quasar. After careful PSF subtraction, only a few compact features were seen, which did not show excess emission in H- $\alpha$  compared to the continuum. The non-detections imply  $3 \sigma$  upper limits on the SFRs of 1.3 – 4.0  $M_{\odot} \text{ yr}^{-1}$ . These limits are much tighter than those reached previously (e.g., with ground-based spectroscopy of Bunker et al. 1999). A similar conclusion has also been reached by Bouché et al. (2001) for a  $z \approx 0.7$  DLA.

Recently, we have obtained deep Ly- $\alpha$  images of quasar absorber fields at  $z = 2.3 - 2.6$  using the NASA Goddard Space Flight Center's Fabry Perot (FP) imager at the Apache Point Observatory (APO) 3.5 m telescope (Kulkarni et al. 2003). The FP serves as a tunable narrow-band filter (400-700 km s<sup>-1</sup> FWHM). In integrations of 400-720 minutes per object, we are reaching  $3\sigma$  flux sensitivity of  $1.0 \times 10^{-17}$  erg s<sup>-1</sup> cm<sup>-2</sup>, allowing some of the best existing SFR constraints.

### 3.2. Comparison with Global Star Formation History

Fig. 2 shows a compilation of SFRs vs. redshift data for quasar absorbers from our NICMOS studies and other emission-line studies in the literature. All measurements are normalized to  $q_0 = 0.5$  and  $H_0 = 70$  km s<sup>-1</sup> Mpc<sup>-1</sup>. The curves show the predictions of Bunker et al. (1999), for the cross-section-weighted SFR for large proto-spiral disks (LD5) and sub-galactic pieces in a hierarchical scenario (H5). These calculations are based on the closed-box global SFR model of Pei & Fall (1995), which agrees with the luminosity density of galaxies from the deep imaging surveys such as the HDF.

Many of the data points in Fig. 2 are for candidates that have not been confirmed spectroscopically. But it is clear that the SFRs of a large fraction of the absorption-selected objects lie far below the model predictions. Thus there appears to be a dichotomy between the absorption and emission pictures of the star formation history of galaxies. This discrepancy seems related to the "missing metals problem" noted by Wolfe et al. (2003). Using C II\* absorption, they estimate SFRs per unit area in DLAs to be comparable to the Galactic value, but find the predicted metal density to be far higher than the observations. One possibility is that the SFRs appear to be low because of dust attenuation, which could also make the metallicity-redshift relation appear flatter than it really is (e.g., Kulkarni & Fall 2002 and references therein). Another possibility is that star formation occurs in compact regions. Further spectroscopic and imaging studies, including large samples of radio-selected quasars, are essential to better understand how important dust selection effects are and where DLAs lie in the overall history of metal production and star formation in galaxies.

## 4. Acknowledgments

It is a pleasure to thank my collaborators Drs. S. M. Fall, D. G. York, J. M. Hill, B. Woodgate, P. Palunas, P. Khare, J. Lauroesch, J. W. Truran, D. E. Welty, and Ms. D. Thatte. I am grateful for support from the National Science Foundation grant AST-0206197, NASA / Space Telescope Science Institute grant GO-9441.01 and from the Univ. of South Carolina Research Foundation. Finally, I thank the organizers of this very fruitful Joint Discussion for inviting me.

## References

- Bouché, N., Lowenthal, J. D., Charlton, J. C., Bershad, M. A., Churchill, C. W., & Steidel, C. C. 2001, *ApJ*, 550, 585
- Bunker, A. J., Warren, S. J., Clements, D. L., Williger, G. M., & Hewitt, P. C. 1999, *MNRAS*, 309, 875

- Khare, P. A., Kulkarni, V. P., Lauroesch, J. T., York, D. G., Crotts, A. P. S., & Nakamura, O. 2004, *ApJ*, 616, 86
- Kulkarni, V. P., Huang, K., Green, R. F., Bechtold, J., Welty, D. E., & York, D. G. 1996, *MNRAS*, 279, 197
- Kulkarni, V. P., Fall, S. M. and Truran, J. W. 1997, *ApJ*, 484, L7
- Kulkarni, V. P., Hill, J. M., Schneider, G., Weymann, R. J., Storrie-Lombardi, L. J., Rieke, M. J., Thompson, R. I., & Jannuzi, B. 2000, *ApJ*, 536, 36
- Kulkarni, V. P., Hill, J. M., Schneider, G., Weymann, R. J., Storrie-Lombardi, L. J., Rieke, M. J., Thompson, R. I., & Jannuzi, B. 2001, *ApJ*, 551, 37
- Kulkarni, V. P., & Fall, S. M. 2002, *ApJ*, 580, 732
- Kulkarni, V. P., Palunas, P., Woodgate, B., & York, D. G. 2003, to be submitted
- Lilly, S. J., Le Fevre, O., Hammer, F., & Crampton, D. 1996, *ApJ*, 460, L1
- Lu, L., Sargent, W. L. W., Barlow, T. A., Churchill, C. W., & Vogt, S. S. 1996, *ApJS*, 107, 475
- Madau, P., Ferguson, H. C., Dickinson, M. E., Giavalisco, M., Steidel, C. C., & Fruchter, A. 1996, *MNRAS*, 283, 1388
- Madau, P., Pozzetti, L., & Dickinson, M. 1998, *ApJ*, 498, 106
- Malaney, R. A., & Chaboyer, B. 1996, *ApJ*, 462, 57
- Meyer, D. M., Welty, D. E., & York, D. G. 1989, *ApJ*, 343, L37
- Pei, Y. C., & Fall, S. M. 1995, *ApJ*, 454, 69
- Pei, Y. C., Fall, S. M., & Hauser, M. G. 1999, *ApJ*, 522, 604
- Pettini, M., Smith, L. J., Hunstead, R. W., & King, D. L. 1994, *ApJ*, 426, 79
- Pettini, M., Smith, L. J., King, D. L., & Hunstead, R. W. 1997, *ApJ*, 486, 665
- Pettini, M., Ellison, S. L., Steidel, C. C., & Bowen, D. V. 1999, *ApJ*, 510, 576
- Prochaska, J. X., & Wolfe, A. M. 1999, *ApJS*, 121, 369
- Prochaska, J. X., & Wolfe, A. M. 2000, *ApJ*, 533, L5
- Prochaska, J. X. et al. 2001, *ApJS*, 137, 21
- Prochaska, J. X., & Wolfe, A. M. 2002, *ApJ*, 566, 68
- Prochaska, J. X. et al. 2003, *ApJ*, 595, L9
- Savaglio, S. 2000, *IAUS*, 204, E24
- Somerville, R. S., Primack, J. R., & Faber, S. M. 2001, *MNRAS*, 320, 504
- Tissera, P. B., Lambas, D. G., Mosconi, M. B., & Cora, S. 2001, *ApJ*, 557, 527
- Vladilo, G., Bonifacio, P., Centurión, M., & Molaro, P. 2000, *ApJ*, 543, 24
- Wolfe, A. M. et al. 1995, *ApJ*, 454, 698
- Wolfe, A. M., Gawiser, E., & Prochaska, J. X. 2003, *ApJ*, 593, 235